Am. J. Hum. Genet. 77:389–407, 2005

Susceptibility Genes for Age-Related Maculopathy on Chromosome 10q26

Johanna Jakobsdottir,[1] Yvette P. Conley,[2,3] Daniel E. Weeks,[1,2] Tammy S. Mah,[4] Robert E. Ferrell,[2] and Michael B. Gorin[2,4]

Departments of [1]Biostatistics and [2]Human Genetics, Graduate School of Public Health, [3]Department of Health Promotion and Development, School of Nursing, and [4]UPMC Eye Center, Department of Ophthalmology, School of Medicine, University of Pittsburgh, Pittsburgh

On the basis of genomewide linkage studies of families affected with age-related maculopathy (ARM), we previously identified a significant linkage peak on 10q26, which has been independently replicated by several groups. We performed a focused SNP genotyping study of our families and an additional control cohort. We identified a strong association signal overlying three genes, *PLEKHA1*, *LOC387715*, and *PRSS11*. All nonsynonymous SNPs in this critical region were genotyped, yielding a highly significant association ($P < .00001$) between *PLEKHA1/LOC387715* and ARM. Although it is difficult to determine statistically which of these two genes is most important, SNPs in *PLEKHA1* are more likely to account for the linkage signal in this region than are SNPs in *LOC387715*; thus, this gene and its alleles are implicated as an important risk factor for ARM. We also found weaker evidence supporting the possible involvement of the *GRK5/RGS10* locus in ARM. These associations appear to be independent of the association of ARM with the Y402H allele of complement factor H, which has previously been reported as a major susceptibility factor for ARM. The combination of our analyses strongly implicates *PLEKHA1/LOC387715* as primarily responsible for the evidence of linkage of ARM to the 10q26 locus and as a major contributor to ARM susceptibility. The association of either a single or a double copy of the high-risk allele within the *PLEKHA1/LOC387715* locus accounts for an odds ratio of 5.0 (95% confidence interval 3.2–7.9) for ARM and a population attributable risk as high as 57%.

Introduction

Age-related maculopathy (ARM), or age-related macular degeneration (ARMD-1 [MIM 603075]), is a leading cause of central blindness in the elderly population, and numerous studies support a strong underlying genetic component to this complex disorder. Genomewide linkage scans performed using large pedigrees, affected sib pairs, and, more recently, discordant sib pairs have identified a number of potential susceptibility loci (Klein et al. 1998; Weeks et al. 2000; Majewski et al. 2003; Schick et al. 2003; Seddon et al. 2003; Abecasis et al. 2004; Iyengar et al. 2004; Kenealy et al. 2004; Schmidt et al. 2004; Weeks et al. 2004; Santangelo et al. 2005). Our genomewide linkage screen strongly implicated the 10q26 region as likely to contain an ARM gene (Weeks et al. 2004); this region has also been supported by many other studies and was the top-ranked region in a recent meta-analysis (Fisher et al. 2005). Recently, three studies (Edwards et al. 2005; Haines et al. 2005; Klein et al. 2005) identified an allelic variant in the complement factor H gene (*CFH* [MIM 134370]) as responsible for the linkage signal seen on chromosome 1 and as the variant accounting for a significant attributable risk (AR) of ARM in both familial and sporadic cases. We and others have confirmed these findings (Conley et al. 2005; Hageman et al. 2005; Zareparsi et al. 2005*a*). *CFH* has previously been suspected of playing a role in ARM, as a result of the work of Hageman and Anderson (Hageman and Mullins 1999; Johnson et al. 2000, 2001; Mullins et al. 2000; Hageman et al. 2001), who have shown that the subretinal deposits (drusen) that are observed in many patients with ARM contain complement factors. However, until other genes that contribute to ARM are identified, *CFH* remains an isolated piece of the puzzle, implicating the alternative pathway and inflammation as part of the ARM pathogenesis but failing to fully account for the unique pathology that is observed in the eye.

We have expanded our family linkage studies and have also undertaken a case-control association study, using a high-density SNP panel in two regions of linkage on 1q31 and 10q26 that we had previously reported. Our SNP linkage and association results for chromosome 1q31 yielded the same findings as others, confirming that the peak of linkage and the strongest associations with ARM were localized over the *CFH* gene. We have analyzed both our family data and the case-control

Received June 7, 2005; accepted for publication June 29, 2005; electronically published July 26, 2005.

Address for correspondence and reprints: Dr. Michael B. Gorin, Department of Ophthalmology, Eye and Ear Institute Building, 203 Lothrop Street, Room 1027, Pittsburgh, PA 15213. E-mail: gorinmb@upmc.edu

0002-9297/2005/7703-0007$15.00

Table 1

Distribution of Subphenotypes in Patients with Advanced ARM

	No. of Patients from CIDR Families[a]		No. of Patients from Local Families[a]		No. of Local Unrelated Patients	
Subphenotype	With GA	Without GA	With GA	Without GA	With GA	Without GA
With CNV	220 (76)	187	130 (45)	106	71 (17)	59
Without CNV	108	62	57	28	40	26

Note.—The numbers in parentheses are the numbers of individuals with both CNV and GA who were also included in GA group (see text for selection criteria) for OR and AR estimation and association tests.

[a] Counts are based on the set of unrelated cases generated by selecting one type A–affected person from each family (see section "Part III: Interaction and OR Analysis: Unrelated cases").

data on chromosome 10q26 to identify the next major ARM susceptibility–related gene.

Material and Methods

Families and Case-Control Cohort

A total of 612 ARM-affected families and 184 unrelated controls were sent to the Center for Inherited Disease Research (CIDR) for genotyping. Because of possible population substructure, we restricted our analysis to the subset of data from white subjects; we were not able to analyze the set of data from nonwhites separately, because it was too small. The white subset had 594 ARM-affected families, containing 1,443 genotyped individuals, and 179 unrelated controls. The white families contained 430 genotyped affected sib pairs, 38 genotyped affected avuncular pairs, and 52 genotyped affected first-cousin pairs.

A total of 323 white families, 117 unrelated controls, and 196 unrelated cases were also genotyped locally for additional SNPs. The local subset contained 824 genotyped individuals, 298 genotyped affected sib pairs, 23 genotyped affected avuncular pairs, and 38 genotyped affected first-cousin pairs. We used PedStats from the Merlin package (Abecasis et al. 2000) to easily get summary counts on the family data.

Affection-Status Models

We have defined three classification models (types A, B, and C) for the severity of ARM status (Weeks et al. 2004). For simplicity, we have restricted our attention here to individuals affected with "type A" ARM, our most stringent and conservative diagnosis. We used only unrelated controls who were unaffected under all three diagnostic models. Unaffected individuals were those for whom eye-care records and/or fundus photographs indicated either no evidence of any macular changes (including drusen) or a small number (<10) of hard drusen ($\leqslant$50 μm in diameter) without any other retinal pigment epithelial (RPE) changes. Individuals with evidence of large numbers of extramacular drusen were not coded as unaffected.

In our efforts to examine specific ARM subphenotypes, we chose to look at only patients with end-stage disease, either those with evidence of choroidal neovascular membrane (CNV) in either eye or those with geographic atrophy (GA) in either eye. There are a significant number of individuals who have been described as having both GA and CNV, though this is problematic, since, in these cases, it is often difficult to determine whether the GA is secondary to the damage from the CNV or is from the treatment given to limit the CNV growth (i.e., laser, surgery, or photodynamic therapy). Because it is often difficult to discern from photographs or records whether a person had GA in an eye prior to the development of CNV, we included the patients who had both pathologies in the CNV group. However, we allowed only a subset of this overlapping group to be included in the GA group, specifically those who reportedly had GA in one eye that did not have evidence of CNV. Table 1 shows the numbers of individuals in each of our three sets. This approach may have excluded a small proportion of individuals from the GA group who had asymmetric GA prior to the development of CNV in the same eye or who may have had bilateral GA but developed CNV in both eyes.

Pedigree and Genotyping Errors and Data Handling

We used the program PedCheck (O'Connell and Weeks 1998) to check for Mendelian inconsistencies. Since it can be extremely difficult to determine which genotypes within small families are erroneous (Mukhopadhyay et al. 2004), we set all genotypes at each problematic marker to missing within each family containing a Mendelian inconsistency. Mega2 (Mukhopadhyay et al. 2005; see Division of Statistical Genetics Web site) was used to set up files for linkage analysis and for allele-frequency estimation by gene counting.

Allele Frequencies and Hardy-Weinberg Equilibrium

The allele frequencies used in the linkage analyses were estimated, by direct counting, from the unrelated and unaffected controls. All controls were unaffected under all three affection status models. Genotyped spouses who had no children or who had children who were not yet part of the study were combined with the controls for this study. The exact test of Hardy-Weinberg equilibrium (HWE), implemented in Mega2 (Mukhopadhyay et al. 2005), was performed on our SNPs.

We also used Mendel (version 5) (Lange et al. 2001) to estimate allele frequencies directly from the family data, because Mendel properly accounts for relatedness of the subjects while estimating the allele frequencies. Since the majority of the genotyped family members were affected, these estimates were quite close to estimates obtained using our unrelated affected cases.

Genetic Map

We used linear interpolation on the Rutgers combined linkage-physical map (version 2.0) (Kong et al. 2004) to predict the genetic position of the SNPs that were not already present in the Rutgers map. Since the distribution of our SNPs was very dense in the regions of interest, the estimated recombination between several SNPs was zero; for these, we set the recombination to 0.000001. We obtained the physical positions for all our SNPs from the National Center for Biotechnology Information (NCBI) dbSNP database (human build 35).

LD Structure

Ignoring high linkage disequilibrium (LD) between SNPs when performing linkage analysis can result in false-positive findings (Schaid et al. 2002; Huang et al. 2004). Our efforts to take high SNP-SNP LD into account included the following measures. (1) We used the H-clust method (Rinaldo et al. 2005), which is implemented in R (R Development Core Team 2004; see R Project for Statistical Computing Web site), to determine haplotype-tagging SNPs (htSNPs) for linkage analysis. The method uses hierarchical clustering to cluster highly correlated SNPs. After the clustering, the H-clust method chooses a htSNP from each cluster; the htSNP chosen is the SNP that is most correlated with all other SNPs in the cluster. We chose to cluster the SNPs so that each SNP had a correlation coefficient (r^2) >0.5 with at least one htSNP; we used HaploView (Barrett et al. 2005) to get a graphical view of SNP-SNP LD along both chromosomes, and we compared LD estimates of htSNPs with SNPs omitted by H-clust. (2) We performed haplotype-based association analyses using two- and three-SNP moving windows (see "Association Analysis" section).

Linkage Analysis

Two-point analysis.—As in our previous study (Weeks et al. 2004), we computed LOD scores under a single simple dominant model (with disease-allele frequency of 0.0001 and penetrance vector of [0.01, 0.90, 0.90]). Because of the complexities and late onset of the ARM phenotype, only two disease phenotypes were used: "affected under model A" (i.e., "type A–affected") and "unknown." Parametric LOD scores were computed under heterogeneity (HLOD), whereas model-free LOD scores were computed with the linear S_{all} statistic. Both scores were computed using Allegro (Gudbjartsson et al. 2000).

Multipoint analysis ignoring LD.—Since intermarker distances are often very small, LD between SNPs can be high and thus violate the assumption of no LD made by most linkage analysis programs. Multipoint analyses ignoring LD were performed using Allegro (Gudbjartsson et al. 2000). Both HLOD scores and S_{all} statistics were computed. Our main goal in estimating the multipoint linkage curve without properly accounting for LD was not to predict the position of ARM-associated loci but to compare the results with those from analyses in which LD was taken into account.

Multipoint analysis using htSNPs.—When only htSNPs were used for LOD score calculation, the number of SNPs decreased from 679 to 533 on chromosome 1 and from 196 to 159 on chromosome 10. Multipoint linkage analyses were done as described elsewhere (Weeks et al. 2004). The SNPs that were omitted fit well into the SNP-SNP LD structure estimated by HaploView (Barrett et al. 2005).

Association Analysis

To incorporate all cases from the families, we used the new CCREL program (Browning et al. 2005), which permits testing for association with the use of related cases and unrelated controls simultaneously. CCREL was used to analyze SNPs under the linkage peak on chromosomes 1 and 10, to test for association. The CCREL test accounts for biologically related subjects by calculating the effective number of cases and controls. For these analyses, type A–affected family members were assigned the phenotype "affected," unrelated controls were assigned the phenotype "normal," and family members that were not affected with type A ARM were assigned the phenotype "unknown." (The CCREL approach has not yet been extended to permit the simultaneous use of both related cases and related controls.) The effective number of controls for each SNP used for association testing is therefore the number of controls genotyped for that SNP. An allelic test, a haplotype test with a two-SNP sliding window, a haplotype test with a three-SNP sliding window, and a genotype test were

Table 2

Summary of Statistical Analyses and Sample Sizes in Parts I–III

Part and Analysis	Set of SNPs, Method, and Sample Used	Results Shown in
I:		
htSNP selection	CIDR SNPs, 179 controls	...
SNP-SNP LD	CIDR SNPs, 179 controls	Figs. 4 and 6
Linkage	CIDR SNPs and htSNPs, 594 ARM-affected families	Figs. 3 and 5
Allele frequencies	Mendel v5 for 594 ARM-affected families; counting for 179 controls	Table 5
CCREL	CIDR SNPs, 594 ARM-affected families and 179 controls	Table 5
GIST	594 ARM-affected families split into 734 typed nuclear families	Table 5
II:		
Allele frequencies	All SNPs (CIDR and local); Mendel v5 for 323 ARM-affected families; counting for 117 controls	Table 6
CCREL	CIDR SNPs and local SNPs, 323 families and 117 controls	Table 6
GIST	323 ARM-affected families split into 407 typed nuclear families	Table 6
SNP-SNP LD	CIDR and local SNPs, 117 unrelated controls	Fig. 2
III:		
Interaction by GIST	See GIST in I and II above	Tables 5 and 6
Logistic regression	CIDR SNPs, 577 cases and 179 controls	Table 7
OR and AR	CIDR SNPs, 577 cases and 179 controls; local SNPs, 517 cases (321 familial, 196 sporadic) and 117 controls	Table 8
OR and AR of subtypes:		
CIDR SNPs	For CNV, 407 cases and 179 controls; for GA, 184 cases and 179 controls	Table 9
Local SNPs	For CNV, 366 cases and 117 controls; for GA, 159 and 117 controls	Table 9

performed. We used the CCREL R package for analysis, as provided by Browning et al. (2005).

GIST Analysis

To explore which allele/SNP contributes the most to the linkage signal, we performed the genotype–identity by descent (IBD) sharing test (GIST) using our locally genotyped SNPs and significant SNPs from the CCREL test that are located around the linkage peaks on chromosomes 1 and 10. GIST determines whether an allele, or another allele in LD with it, accounts in part for the observed linkage signal (Li et al. 2004). Weights were computed for each affected sibship under three different disease models (recessive, dominant, and additive); these weights are unbiased under the null hypothesis of no disease-marker association. The correlation between the family weight variable and the nonparametric linkage (NPL) score is the basis of the test statistic. Since the GIST method is currently applicable only to affected sib pair families, we split our families into their component nuclear families before computing the NPL scores. Since we do not know the underlying disease model, we performed tests using three different disease models (recessive, dominant, and additive) and then took the maximum result, using a *P* value that was adjusted for multiple testing over the three models.

Tripartite Analyses

Our analyses were performed in three sequential steps. First, we analyzed the set of data that had been genotyped at CIDR. Second, after locally genotyping eight additional SNPs in the *PLEKHA1/LOC387715/PRSS11* region on chromosome 10, we then analyzed the locally genotyped data set. Note that all of the known nonsynonymous SNPs in the region from *PLEKHA1* (MIM 607772) through *PRSS11* (MIM 602194) were investigated. Because these two data sets differ in size and composition, it is most straightforward to analyze them separately (table 2). Allele-frequency estimation, CCREL association testing, and GIST analysis were performed on both of these (overlapping) data sets, as described above. Third, we tested for interaction between the chromosome 1 and chromosome 10 regions and examined whether or not the risk differed as a function of the presence of either GA or CNV.

Part I: Analysis of CIDR SNPs

To identify the responsible gene on chromosome 10q26, the CIDR performed high-density custom SNP genotyping of 612 ARM-affected families and 184 unrelated controls with the use of 199 SNPs spanning 13.4 Mbp (26.7 cM), from *rs7080289* through *rs6597818* (nucleotide position: 115094788–128517320 bp), which spans our region of interest. For our analysis, we used 196 SNPs; 3 were skipped because of a lack of polymorphism in the controls (when this was checked within the family data, the less common allele was extremely rare and was only present in heterozygotes). In addition, 684 SNPs spanning 45.7 Mbp (47.1 cM) on chromosome 1q31, from *rs723858* through *rs653734* (nucleotide position: 169749920–215409007 bp), were also genotyped; 5 SNPs were skipped because of a lack of polymorphism in the controls—the less common allele was either not present or very rare and, in the family

data, was only present in heterozygotes. Table 3 shows the correspondence between our allele labels and the actual alleles, and, for nonsynonymous SNPs, the amino acid change.

Part II: Analysis of Locally Genotyped SNPs

We genotyped eight additional SNPs on chromosome 10 that overlie three susceptibility genes, *PLEKHA1* (*rs12258692, rs4405249,* and *rs1045216*), *LOC387715* (*rs10490923, rs2736911,* and *rs10490924*), and *PRSS11* (*rs11538141* and *rs1803403*). This genotyping effort included all of the nonsynonymous SNPs that have been reported for these genes in the NCBI databases (see fig. 1). As part of another study (Conley et al. 2005), we genotyped two *CFH* variants (*rs10922093* and *rs1061170*), which we have used here as well. Genotyping of additional SNPs under the *GRK5/RGS10* (MIM 600870/MIM 602856) locus is in process. Genotype data for *rs12258692, rs1803403,* and the newly characterized SNP *rs4405249* (which is 1 base 3′ of *rs12258692*) were collected by sequencing (Rexagen) and were analyzed using Sequencher software (Gene Codes). Genotype data for *rs11538141, rs2736911, rs10490923*, and *rs10490924* were collected using RFLP. The primers, amplification conditions, and restriction endonucleases, where appropriate, for SNPs that were genotyped by sequencing or RFLP can be found in table 4. Genotype data for *rs1045216* were collected using a 5′ exonuclease Assay-on-Demand TaqMan assay (Applied Biosystems). Amplification and genotype assignments were conducted using the ABI 7000 and SDS 2.0 software (Applied Biosystems). Two unrelated CEPH samples were genotyped for each variant and were included on each gel and in each TaqMan tray, to assure internal consistency in genotype calls. Additionally, double-masked genotyping assignments were made for each variant and were compared, and each discrepancy was addressed using raw data or regenotyping. Table 3 shows the correspondence between our allele labels and the actual alleles and, for nonsynonymous SNPs, the amino acid change.

Part III: Interaction and OR Analysis

Unrelated cases.—No unrelated cases were genotyped by CIDR, but 196 unrelated cases were genotyped locally for our additional SNPs. For computation of odds ratios (ORs) and for interaction analyses (see below), we chose to generate a set of unrelated cases by drawing one type A–affected person from each family. A total of 321 locally genotyped families had at least one type A–affected person. If a family had more than one type A–affected person, we chose the person who had the most complete genotyping at the Y402H variant (*rs1061170*) and three CIDR SNPs representative of *CFH, GRK5,* and *PLEKHA1*: *rs800292* (*CFH*), *rs1537576* (*GRK5*), and *rs4146894* (*PLEKHA1*; *rs4146894* also represents *LOC387715,* because of high LD with *rs10490924*) (see fig. 2). If they could not be distinguished by the number of genotyped SNPs, we chose the person who developed the disease at the youngest age, or, if more than one shared the earliest age at onset, we selected one type A–affected individual at random from those with the most SNPs genotyped and the earliest age at onset. A total of 577 CIDR families had at least one type A–affected person; 321 of these families were also genotyped locally, and the type A–affected person was the same one chosen for the local set. For the remaining 256 families, we based our selection on the same criteria described above, except that only *rs800292* (*CFH*), *rs1537576* (*GRK5*), and *rs4146894* (*PLEKHA1*) were used to identify the person with the most complete genotyping.

Table 3

Allele Labeling

The table is available in its entirety in the online edition of *The American Journal of Human Genetics*.

Analysis of interaction with CFH.—We investigated possible interaction between *CFH* on chromosome 1 and the genes on chromosome 10 by using GIST to test whether SNPs in *CFH* are associated with the linkage signal on chromosome 10 and whether SNPs on chromosome 10 are associated with the linkage signal on chromosome 1. We did this by using weights from SNPs on one chromosome and family-based NPLs from the other.

We also used logistic regression to evaluate different interaction models and to test for interaction by use of the approach described by North et al. (2005). In this approach, many different possible models of the interactions, allowing simultaneously for additive and dominant effects at both of the loci, are fit, and relative likelihoods of the different models are compared to draw inferences about the most likely and parsimonious model. As described elsewhere (North et al. 2005), the fitted models include a MEAN model, in which only the mean term is estimated; ADD1, ADD2, and ADD models, which assume an additive effect at one or both loci; DOM1, DOM2, and DOM models, which additionally incorporate dominance effects; and three further models, ADDINT, ADDDOM, and DOMINT, which allow for interactive effects (for more details, see the work of North et al. [2005]). Since some pairs of these models are not nested, we compared them by using the Akaike information criteria (AIC); in this approach, the model with the lowest AIC is considered to be the best fitting and the most parsimonious. For these analyses, we used the program provided by North and colleagues (2005), after some bugs that we discovered had been fixed; we double-checked our results with our own R program. To maximize the sample size, we chose CIDR SNPs in

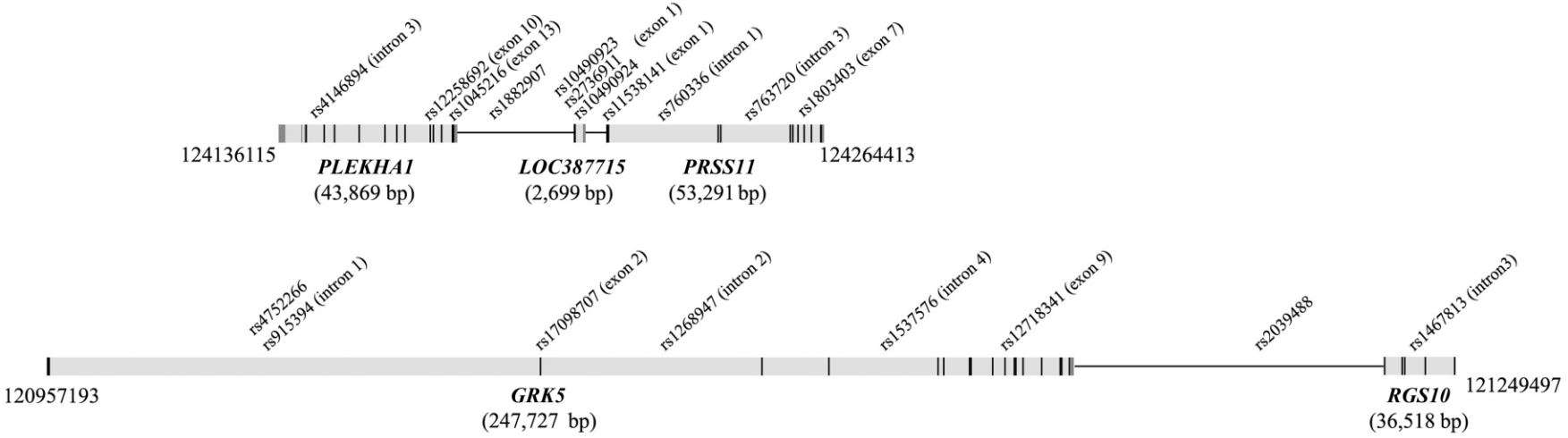

Figure 1 Location of CIDR SNPs and locally genotyped SNPs with respect to candidate genes. Positions, distances, and nucleotide positions along chromosome 10 are derived from NCBI Entrez Gene and dSNP databases.

Table 4

Primers, Annealing Conditions, and Restriction Endonucleases Used for Genotype Data Collection

The table is available in its entirety in the online edition of *The American Journal of Human Genetics*.

high LD with a highly significant nonsynonymous SNP within each gene. The CIDR SNP *rs800292* was chosen to represent *rs10611710* (the Y402H variant of *CFH*), and the CIDR SNP *rs4146894* represented *rs1045216* in *PLEKHA1*. Similarly, we also selected a representative CIDR SNP in *GRK5, RGS10,* and *PRSS11*.

Magnitude of association.—We calculated crude ORs and estimated ARs for SNPs in each gene. The allele that was least frequent in the controls was considered to be the risk allele. AR was estimated using the formula $AR = 100 \times P \times (OR - 1)/[1 + P \times (OR - 1)]$, where OR is the OR and P is the frequency of the risk factor (genotype) in the population, as estimated from the controls. We did this by comparing type A–affected subjects with controls, comparing subjects who had CNV with controls, and comparing subjects who had GA with controls. To have the maximum possible sample size, we used different but overlapping samples for CIDR and locally typed SNPs. A total of 577 cases selected from the families and 179 unrelated cases were used for calculating OR and AR of CIDR SNPs, but 517 cases (of those, 321 are within the 577 CIDR SNP cases) and 117 controls (all within the 179 CIDR SNP controls) were used for calculating the OR and AR on the locally genotyped SNPs.

Multiple-testing issues.—Since we have very strong evidence from previous studies that there is an ARM-susceptibility locus in the chromosome 10q26 region, the analyses performed here were aimed at estimating the location of the susceptibility gene, rather than testing a hypothesis. Multiple-testing issues are most crucial and relevant in the context of hypothesis testing. In estimation, we are simply interested in determining where the signal is strongest. In any event, any correction for multiple testing would not alter the rank order of the results. A Bonferroni correction, which does not account for any correlation between tests due to LD, for 196 tests at the 0.05 level would lead to a significance threshold of $0.05/196 = 0.00026$; correlations due to LD would lead to a larger threshold.

Results

Our analyses were performed in three sequential steps. First, we analyzed the set of data that had been genotyped at CIDR. Second, after locally genotyping eight additional SNPs in the *PLEKHA1/LOC387715/PRSS11* region on chromosome 10, we then analyzed the locally genotyped data set. Allele-frequency estimation, testing for HWE (table 3), CCREL association testing, and GIST testing were performed on both of these (overlapping) data sets, as described above. Third, we tested for interaction between the chromosome 1 and chromosome 10 regions and examined whether or not the risk differed as a function of the presence of GA or CNV.

Part I: Analysis of CIDR SNPs

CIDR linkage results.—The narrow peak of our S_{all} linkage curve obtained using the 159 htSNPs on chromosome 10 suggests that there might be an ARM gene in the *GRK5* region (marked "G" in fig. 3, right panel); *rs1537576* in *GRK5* had a two-point S_{all} of 1.87, whereas the largest (across our whole region) two-point S_{all} of 3.86 occurred at *rs555938,* 206 kb centromeric of *GRK5*. Several elevated two-point nonparametric S_{all} LOD scores and our highest HLOD score drew attention to the *PLEKHA1/LOC387715/PRSS11* region (marked "P" in fig. 3). In this region, SNP *rs4146894* in *PLEKHA1* had a two-point S_{all} of 3.34 and the highest two-point HLOD of 2.66, whereas SNPs *rs760336* and *rs763720* in *PRSS11* had two-point S_{all} values of 2.69 and 2.23, respectively. However, the 1-unit support interval is large (10.06 cM) (fig. 3), and so localization from the linkage analyses alone is rather imprecise.

We also explored the effect of failing to take SNP-SNP LD into account, by comparing the multipoint scores computed using all SNPs (fig. 3, left panel) with those computed using only the htSNPs (fig. 3, right panel). Two of the peaks found using all SNPs (referred to as "false peaks"; marked "F" in fig. 3, left panel) almost vanish completely when using only htSNPs; interestingly, these two peaks lie within haplotype blocks (fig. 4*A* and 4*B*), whereas the LD around our highest multi- and two-point LOD scores is low (fig. 4*C*), indicating the importance of taking LD into account when performing linkage analysis.

Our linkage results on chromosome 1 gave three peaks with $S_{all} > 2$, and only one of those peaks was observed when we restricted our analysis to htSNPs (fig. 5). This remaining peak overlies *CFH* and includes two SNPs with very high two-point S_{all} and HLOD scores: *rs800292,* a nonsynonymous SNP in *CFH,* had an S_{all} of 1.53 and an HLOD of 2.11, whereas SNP *rs1853883,* 165 kb telomeric of *CFH,* had an S_{all} of 4.06 and an HLOD of 3.49. These results strongly support earlier findings of *CFH*'s involvement in ARM (Conley et al. 2005; Edwards et al. 2005; Hageman et al. 2005; Haines et al. 2005; Klein et al. 2005; Zareparsi et al. 2005*a*). The vanishing peaks (marked "F" in fig. 5, left panel) that we saw when we used all of our SNPs in the linkage analysis are located within strong haplotype blocks (fig. 6*A* and 6*B*), whereas the LD under the *CFH* peak is relatively low (fig. 6*C*).

CIDR association results.—For finer localization than

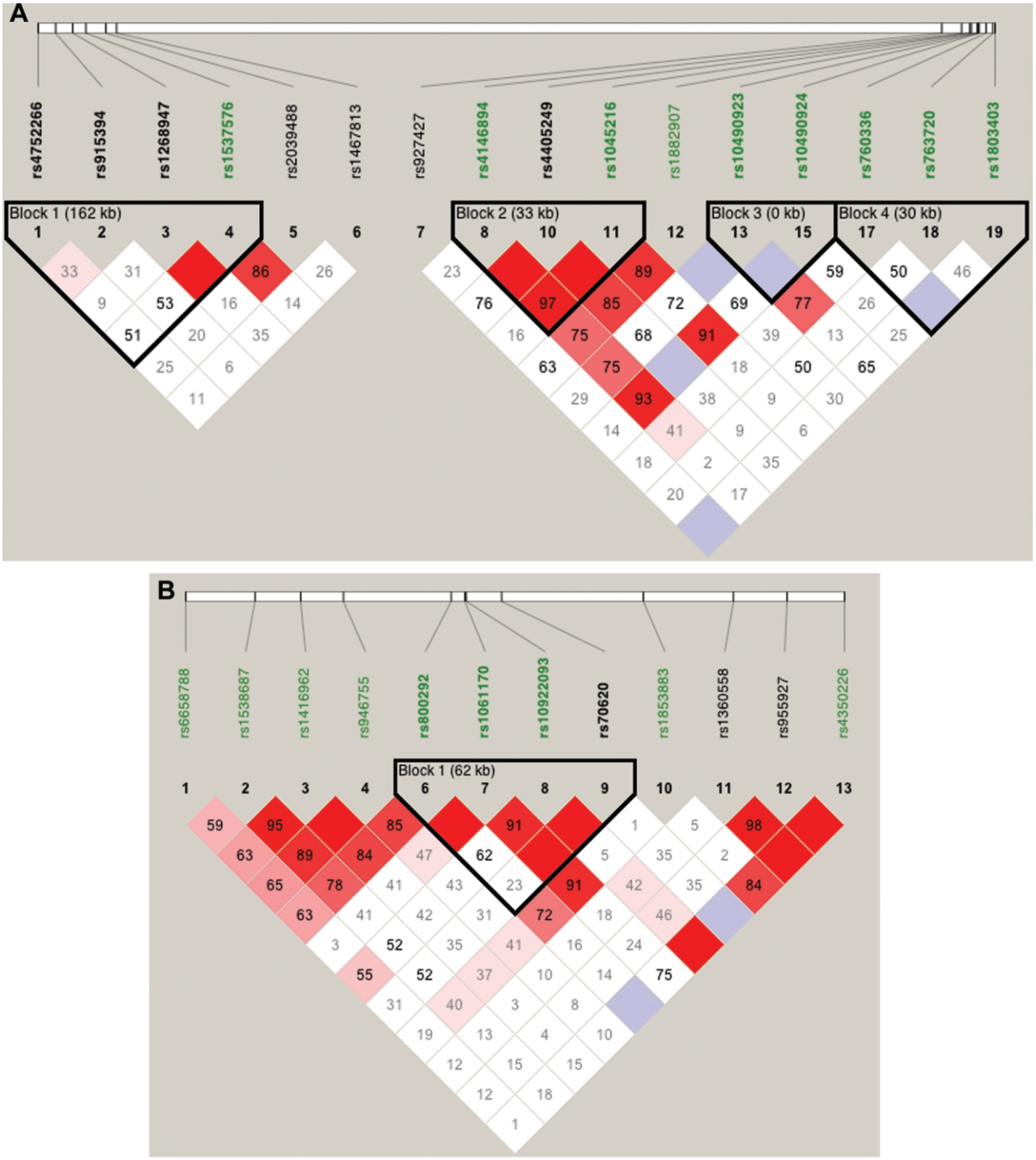

Figure 2 *A*, LD patterns in *GRK5* (Block 1), *RGS10* (SNP 6), *PLEKHA1* (Block 2), *LOC387715* (Block 3), and *PRSS11* (Block 4). *B*, LD patterns in *CFH* (Block 1). Squares shaded pink or red indicate significant LD between SNP pairs (bright red indicates pairwise $D' = 1$), white squares indicate no evidence of significant LD, and blue squares indicate pairwise $D' = 1$ without statistical significance. Significant SNPs from the CCREL allele test are highlighted in green (see table 6). Three SNPs (*rs6428352*, *rs12258692*, and *rs11538141*) were not included, because of very low heterozygosity, and one SNP (*rs2736911*) was not included, because it was uninformative. Note that the blocks were drawn to show clearly the position of the genes and do not represent haplotype blocks.

can be obtained by linkage, we turned to association analyses (which were very successful in discovering *CFH* on chromosome 1). Here, we performed association analyses using the CCREL approach (Browning et al. 2005), which permitted the simultaneous use of our unrelated controls and all of our related familial cases by appropriately adjusting for the relatedness of the cases. In the CIDR sample on chromosome 10, within our linkage peak, we found a cluster of four adjacent SNPs with very small *P* values (*rs4146894, rs1882907, rs760336,* and *rs763720*) that overlies three genes: *PLEKHA1, LOC387715,* and *PRSS11.* Our strongest CCREL results on chromosome 10 were for SNP *rs4146894* in *PLEKHA1* (table 5). The moving-window haplotype analyses using three SNPs at a time resulted in very small *P* values across the whole *PLEKHA1* to *PRSS11* region (table 5). The association testing also generated some moderately small *P* values in the *GRK5* region, which is where our highest evidence of linkage occurred.

We performed the CCREL on 56 SNPs spanning the linkage peak on chromosome 1 and found two highly significant SNPs (*rs800292* and *rs1853883*) that overlie *CFH* (table 5). The moving-window haplotype analyses, performed using two and three SNPs at a time, resulted in extremely low *P* values across the whole *CFH* gene (table 5), which supports earlier findings of strong association between *CFH* and ARM.

CIDR GIST results.—When GIST was performed on the CIDR data set, the two smallest *P* values in chromosome 10q26 (.006 and .004) occurred in the *GRK5/RGS10* region, whereas the third smallest *P* value (.008) occurred in *PLEKHA1* (table 5). All four SNPs in the *GRK5* gene have small GIST *P* values. The GIST results suggest that both *GRK5* and *PLEKHA1* contribute significantly to the linkage signal on chromosome 10 and that *CFH* contributes to the linkage signal on chromosome 1. Neither of the two SNPs in *PRSS11* contributes significantly to the linkage signal on chromosome 10. There was no evidence that the genes on chromosome 10 were related to the linkage signal seen on chromosome 1.

PART II: Analysis of Locally Genotyped SNPs

Local association results.—After additional SNPs were typed locally, the allele and genotype test generated extremely small *P* values for each of the three genes *PLEKHA1, LOC387715,* and *PRSS11* (table 6). The moving-window haplotype analyses with three SNPs resulted in very small *P* values across the entire *PLEKHA1/LOC387715/PRSS11* region (table 6). Thus, although association implicates the *PLEKHA1/LOC387715/PRSS11* region, it does not distinguish between these genes.

Local GIST results.—Of the three genes *PLEKHA1, LOC387715,* and *PRSS11,* GIST most strongly implicated *PLEKHA1* (table 6). It also generated a small *P* value for *rs10490924* in *LOC387715,* but this SNP is in high LD with the *PLEKHA1* SNPs (see fig. 2*A*). When the locally typed data set was used, GIST did not generate any significant results for *PRSS11,* similar to the nonsignificant results observed in the larger CIDR sample. This implies that *PLEKHA1* (or a locus in strong LD with it) is the most likely to be involved in ARM, and therefore *LOC387715* remains a possible candidate locus.

For a fair assessment of which SNP accounts for the linkage signal across the region, the NPLs were computed using only the locally genotyped families. This permitted us to compare the *PLEKHA1/LOC387715/PRSS11* results (table 6) directly with the *GRK5/RGS10* results. For the locally typed data set, the GIST results for *GRK5* are also interesting, with modest *P* values of the same magnitude as the *P* values we got from applying GIST to *CFH* (table 6). However, note that the *P* values are not as small as those seen when the CIDR data set was analyzed. Since all of the SNPs in the *GRK5* region are CIDR SNPs, this difference is solely a function of sample size, because the locally typed data set is smaller than the CIDR data set (see table 2).

Part III: Interaction and OR Analyses

GIST results.—We did not see any strong evidence of an interaction between the chromosome 1 and chromosome 10 regions, by use of GIST. When the CIDR data set was used to test whether SNPs on chromosome 10 contribute to the linkage signal on chromosome 1 (see GIST, NPL 1, in table 5), only *rs763720* in *PRSS1* gave a *P* value <.05; however, *rs763720* does not contribute significantly to the linkage signal on chromosome 10, which makes this *P* value less convincing. When we used the local data set, one *GRK5* variant (*rs1537576*), which was not significant in the larger CIDR data set, gave a *P* value <.05. Similarly, we did not see evidence that SNPs within *CFH* contribute to the linkage signal on chromosome 10; only one SNP (*rs955927*) gave a *P* value <.05—this SNP, however, is not in the *CFH* gene and is not in strong LD (see fig. 2*B*) with any SNPs in *CFH*.

Logistic regression results.—The logistic regression results (table 7) suggest that an additive model including the variants from *CFH* and *PLEKHA1* is the best model for predicting case-control status; this indicates that both genes are important to the ARM phenotype. The AIC criteria also suggest that an additive model including an additive interaction term is the next best model (table 7); however, the interaction term is not significant ($P = .71$). We obtain similar results for interaction be-

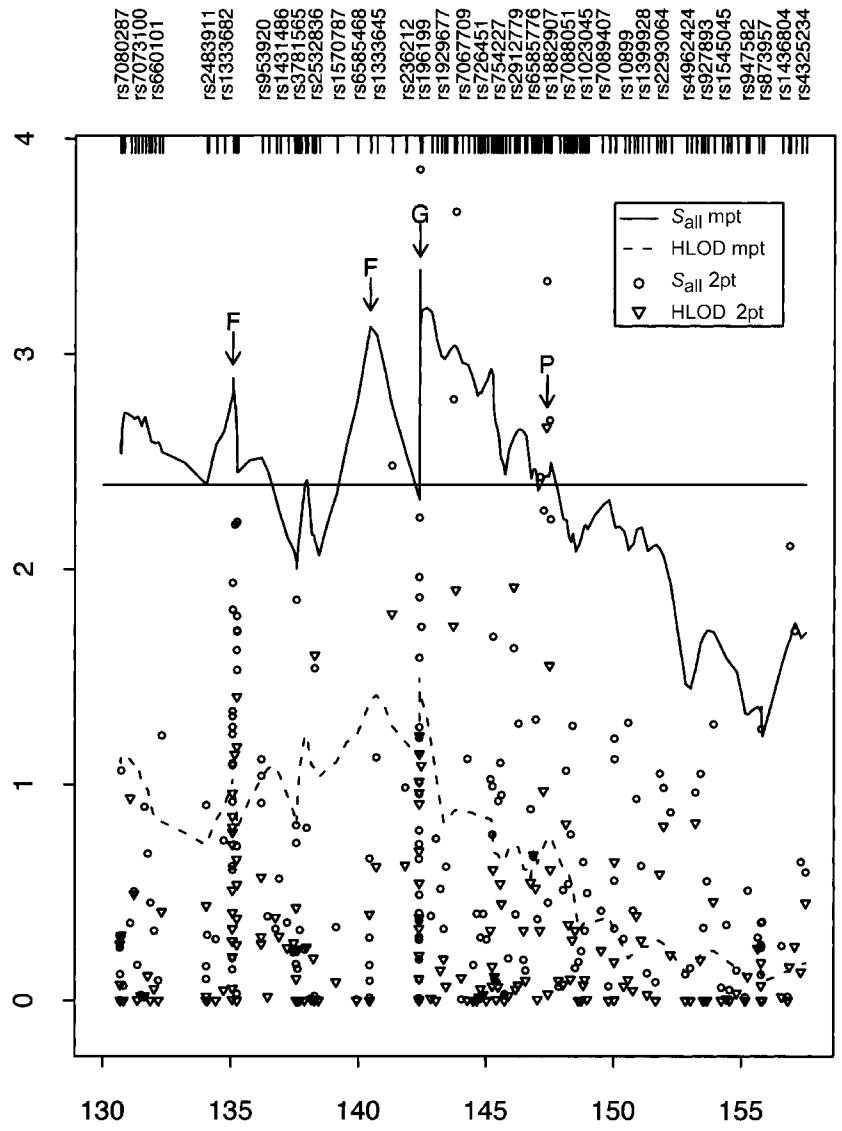

Chromosome 10: 196 SNPs

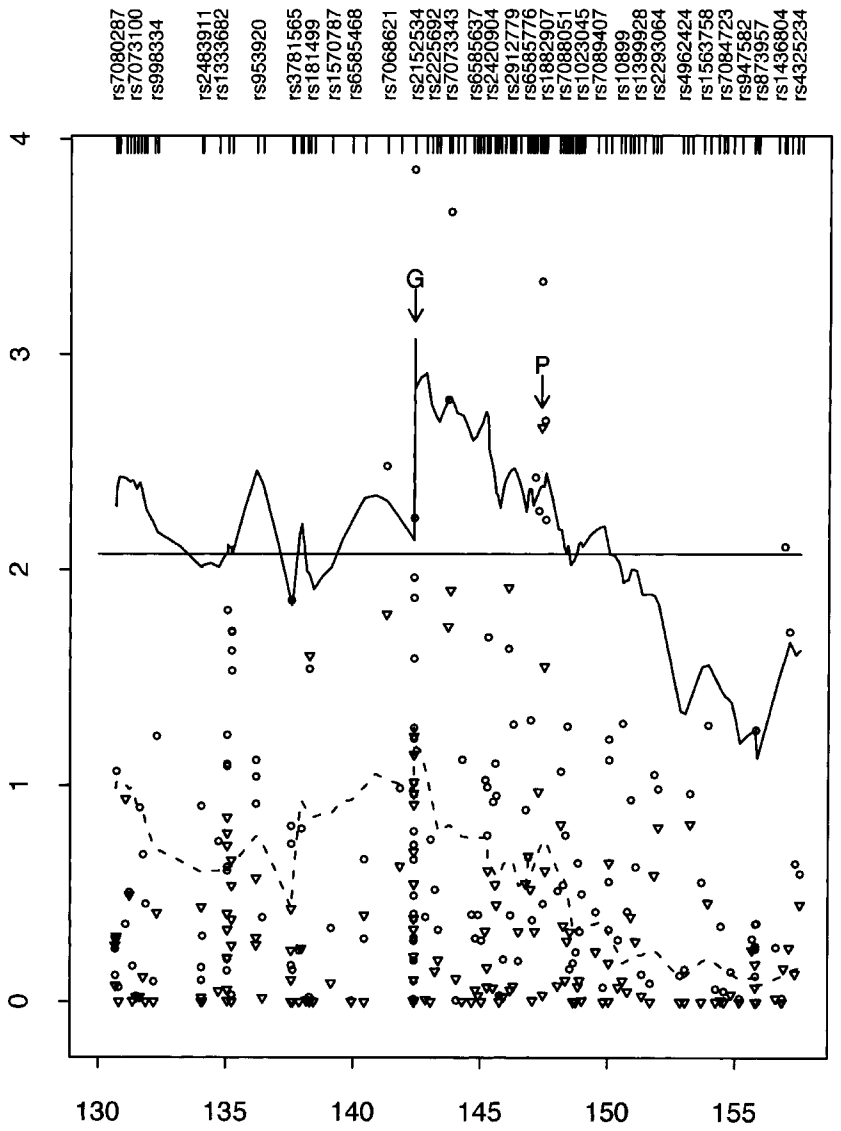

Chromosome 10: 159 SNPs (H–clust 0.5)

tween *CFH* and *PRSS11,* where the additive model including both variants appears to be the best model. Within the *GRK5/RGS10* region, a model with the *CFH* SNP alone is the best-fitting model, which suggests that the prediction of case-control status with *CFH* genotype does not improve by the addition of either the *GRK5* or *RGS10* variant to the model.

OR and AR.—We estimated the magnitude of association by calculating OR and AR values; the significant associations we saw (table 8) are, not surprisingly, consistent with the results from the CCREL tests in parts I and II. Our two most significant SNPs in the *PLEKHA1/LOC387715* region are SNPs *rs4146894* (*PLEKHA1*) and *rs10490924* (*LOC387715*); the two tests are highly correlated because the LD between those SNPs is very high ($D' = 0.93$) (see fig. 2*A*). The third most significant SNP (*rs1045216*) in the chromosome 10 region is a nonsynonymous SNP in *PLEKHA1* and in high LD with both *rs4146894* ($D' = 0.97$) and *rs10490924* ($D' = 0.91$).

We obtained results and OR and AR values (table 8) similar to those that others have reported for the *CFH* gene. The three most significant SNPs were *rs1061170* (Y402H variant), *rs800292* (in *CFH*), and *rs1853883* (in strong LD with *rs1061170*; $D' = 0.91$).

The magnitude of the association we saw within *PLEKHA1/LOC387715* is very similar to the level of association seen between *CFH* and ARM; both loci result in extremely low *P* values ($P < .0001$). The OR and AR values were also similar—the dominant OR was 5.29 (95% CI 3.35–8.35) within *CFH* and 5.03 (95% CI 3.2–7.91) within *PLEKHA1/LOC387715,* and the dominant AR for *CFH* and *PLEKHA1/LOC387715* was 68% and 57%, respectively.

Subphenotype analyses.—We estimated ORs and ARs for patients with exudative disease versus controls and for patients with GA versus controls (table 9). ORs and corresponding *P* values yielded similar findings to those of the allele test of CCREL (tables 5 and 6). We found no major differences between the ORs for the presence of either GA or CNV.

Discussion

Our linkage studies of families with ARM have consistently identified the chromosome 1q31 and chromosome 10q26 loci, in addition to several other loci. Multiple linkage studies have replicated this finding; thus, we undertook a focused SNP analysis of both regions, using ARM-affected families as well as unrelated affected individuals and controls. We confirmed the strong association of chromosome 1q31 with *CFH* that has been reported by others (see also Conley et al. [2005]), and we have shown, for the first time, that SNPs in *CFH* significantly account for the linkage signal. Interestingly, our smallest GIST *P* value (<.001) was for *rs1853883* (which has a high D' of 0.91 with the Y402H variant) and not for the presumed "disease-associated" Y402H variant itself. This raises the possibility that we may still have to consider other possible ARM-related variants within the *CFH* gene and that these may be in high LD with Y402H.

Our studies of chromosome 10q26 have implicated two potential loci: (1) a very strongly implicated locus that includes three tightly linked genes, *PLEKHA1, LOC387715,* and *PRSS11,* and (2) a less strongly implicated locus comprising two genes, *GRK5* and *RGS10* (fig. 1). The GIST analysis does not support *PRSS11* as the ARM-related gene, but it does not completely exclude it as a potential candidate. *PLEKHA1* has the lowest GIST-derived *P* values, whereas *LOC387715* harbors the SNP with the strongest association signal and the highest ORs. With the high LD between SNPs in *LOC387715* and *PLEKHA1,* one cannot clearly distinguish between these genes by statistical analyses alone. However, it is clear that the magnitude of the impact of the *PLEKHA1/LOC387715* locus on ARM is comparable to that which has been observed for the *CFH* locus. As in recent studies (Edwards et al. 2005; Haines et al. 2005; Klein et al. 2005), we have found, in our case-control population, that the *CFH* allele (either heterozygous or homozygous) accounts for an OR of 5.3 (95% CI 3.4–8.4) and a significant population AR of 68%. In the same fashion, the high-risk allele within the *PLEKHA1/LOC387715* locus accounts for an OR of 5.0 (95% CI 3.2–7.9) and an AR of 57% when both heterozygous and homozygous individuals are considered. As noted by Klein et al. (2005), unless

The figure is available in its entirety in the online edition of *The American Journal of Human Genetics.*

Figure 4 LD patterns on chromosome 10 based on analysis of 196 CIDR SNPs and 179 unrelated controls. The legend is available in its entirety in the online edition of *The American Journal of Human Genetics.*

Figure 3 Two-point (2pt) and multipoint (mpt) linkage results on chromosome 10. The panel on the left summarizes the results when all SNPs were used for analysis. The panel on the right summarizes the results when only htSNPs were used. The peaks marked "F" represent likely false peaks due to high SNP-SNP LD, whereas the peaks marked "G" and "P" correspond to the loci containing *GRK5* and *PLEKHA1,* respectively. The horizontal lines indicate the 1-unit support interval of multipoint S_{all} (i.e., maximum $S_{all} - 1$).

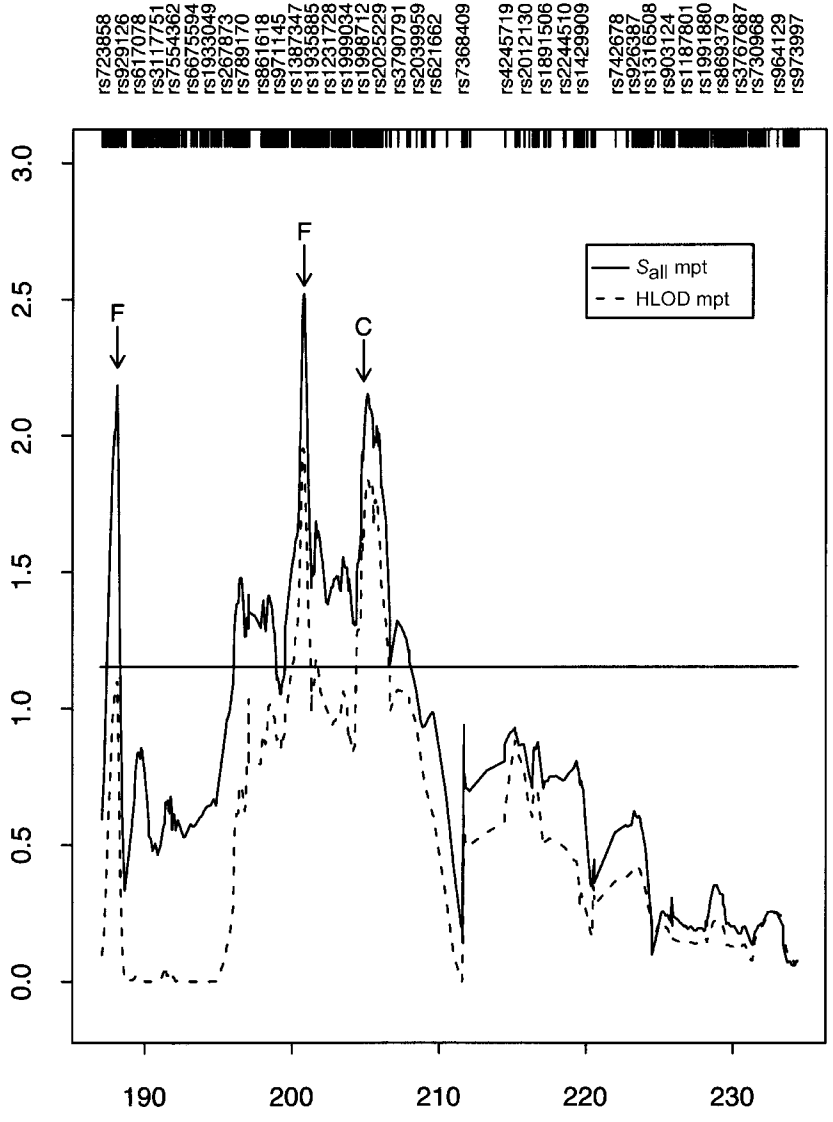

Chromosome 1: 697 SNPs

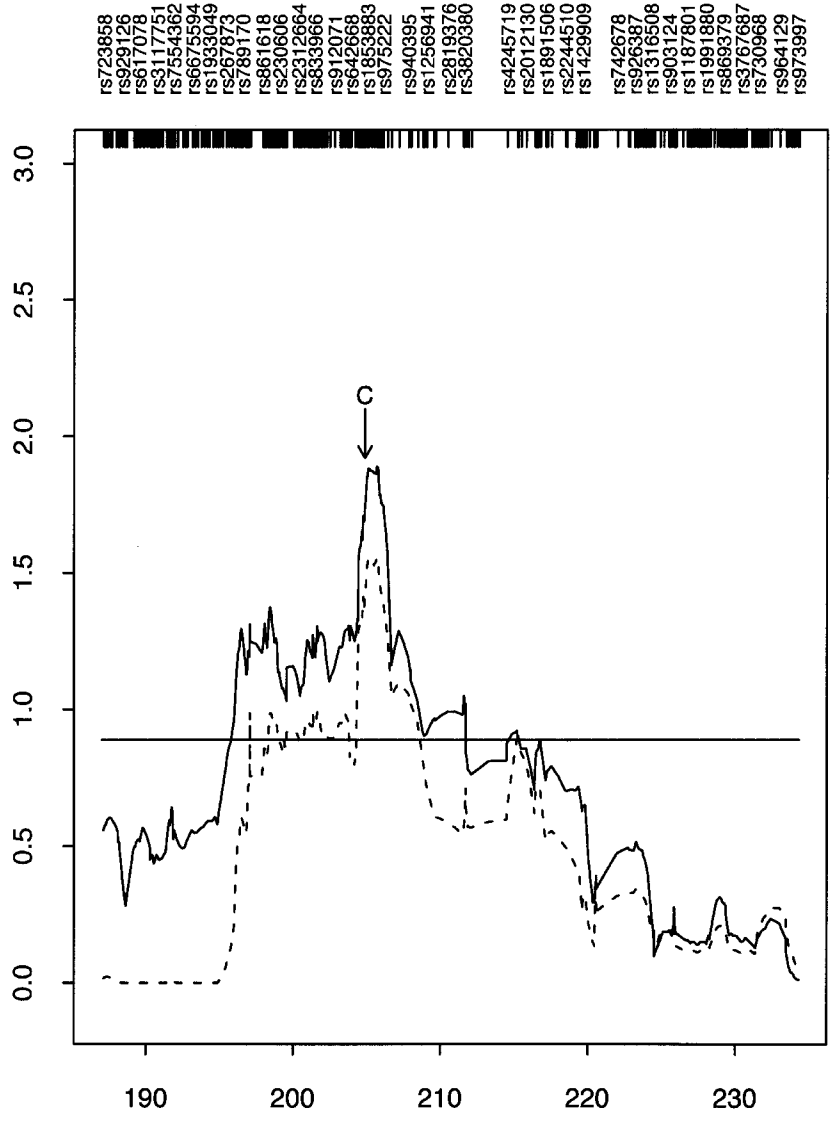

Chromosome 1: 533 SNPs (H–clust 0.5)

the disease is very rare, the OR determined from a case-control study will usually overestimate the equivalent relative risk. Estimates of AR based on ORs for common genetic disorders can misrepresent the extent to which a variant accounts for the population AR. However, if this caution is kept in mind, it is still useful for us to present AR values to allow for relative comparisons and to allow the reader to appreciate that the potential impact of the *CFH* Y402H variant on ARM is comparable to that of the variants observed in the *PLEKHA1/LOC387715* locus.

In the case of *CFH* on chromosome 1, the association data were extremely compelling for a single gene, even though *CFH* is within a region of related genes. In addition to the association data found by multiple independent groups, there is additional biological data to implicate *CFH,* including localization of the protein within drusen deposits of patients with ARM. Thus, we also must consider the biological relevance of the potential ARM-susceptibility genes identified by our studies of chromosome 10q26.

As noted above, the GIST analysis most strongly implicated *PLEKHA1,* particularly when we included the additional nonsynonymous SNPs that we genotyped locally. *PLEKHA1* encodes the protein TAPP1, which is a 404-aa protein with a putative phosphatidylinositol 3,4,5-trisphosphate-binding motif (PPBM), as well as two plectstrin homology (PH) domains. The last three C-terminal amino acids have been predicted to interact with one or more of the 13 PDZ domains of MUPP1 (similar to the PDZ domain within PRSS11). Dowler and colleagues (2000) have shown that the entire TAPP1 protein, as well as the C-terminal PH domain, interacts specifically with phosphatidylinositol 3,4-bisphosphate (PtdIns(3,4)P2) but not with any other phosphoinositides. TAPP1, which has 58% identity with the first 300 aa of TAPP2, shows a fivefold higher affinity for PtdIns(3,4)P2 than does TAPP2, and this binding is nearly eliminated by mutation of the conserved arginine 212 to leucine within the PPBM region (which is part of the second PH domain). The most well-defined role for TAPP1 (and its relatives, Bam32 and TAPP2) has been as an activator of lymphocytes. PtdIns(3,4)P2 is preferentially recruited to cell membranes when lipid phosphatase (SHIP) is activated along with PI3K (phosphatidyl inositol 3-kinase). SHIP is responsible for the dephosphorylation of PIP3 to PtdIns(3,4)P2. SHIP is a negative regulator of lymphocyte activation, and thus TAPP1 and TAPP2 may be crucial negative regulators of mitogenic signaling and of the PI3K signaling pathway. Thus, one can envision a role in the eye for *PLEKHA1* and its protein, TAPP1, in modifying local lymphocyte activation, consistent with the hypothesis that ARM is closely linked to an inflammatory process.

The figure is available in its entirety in the online edition of *The American Journal of Human Genetics.*

Figure 6 LD patterns on chromosome 1 based on analysis of 679 CIDR SNPs and 179 unrelated controls. The legend is available in its entirety in the online edition of *The American Journal of Human Genetics.*

However, we need to still consider the biological plausibility of the other two candidate genes within this locus, *LOC387715* and *PRSS11.* Little is known regarding the biology of *LOC387715,* except that its expression appears to be limited to the placenta. Our own reverse transcription experiments with human retinal RNA have confirmed the expression of *PLEKHA1* and *PRSS11,* but we have not detected *LOC387715* transcripts in the retina under standard conditions, even though we confirmed its expression with placental RNA (data not shown). However, we cannot exclude the possibility that *LOC387715* is expressed at very low levels in the retina or retinal pigment epithelium or that its expression in nonocular tissues, such as dendritic cells or migrating macrophages, could be a factor in the pathogenesis of ARM.

PRSS11 is one of the genes of the mammalian high temperature requirement A (HtrA) serine protease family, which has a highly conserved C-terminal PDZ domain (Oka et al. 2004). These secretory proteases were initially identified because of their homologies to bacterial forms that are required for survival at high temperatures and molecular chaperone activity at low temperatures. The ATP-independent serine protease activity is thought to degrade misfolded proteins at high temperatures. The mammalian form, HtrA1, has been shown to be selectively stimulated by type III collagen alpha 1 C propeptide, in contrast to HtrA2 (Murwantoko et al. 2004). Type III collagen is a major constituent (35%–39% of the total collagen) in Bruch membrane and is also present in small amounts in the retinal microvascular basement membranes. Developmental studies have reported ubiquitous expression of HtrA1, but with temporal and spatial specificities that coincide with

Figure 5 Multipoint linkage results for chromosome 1. The panel on the left summarizes results when all SNPs were used for analysis, and the panel on the right summarizes results when only htSNPs were used. The peaks marked "F" represent likely false peaks due to high SNP-SNP LD, whereas the peak marked "C" corresponds to the *CFH* gene. The horizontal lines indicate the 1-unit support interval of multipoint S_{all} (i.e., maximum S_{all} over $CFH - 1$).

Table 5

CCREL, GIST, and Allele-Frequency Estimation for Families and Controls Typed at CIDR

				P Value for Test					
		Frequency in			Moving-Window Haplotype Test			GIST	
SNP	Gene	Families (n = 594)	Controls (n = 179)	Allele Test	With 2 SNPs	With 3 SNPs	Genotype Test	NPL 10	NPL 1
rs6658788		.460	.489	.37312	***.01616***	***.00778***	.44415	.106	.055
rs1538687		.234	.307	.00178	***.00206***	***.00674***	***.0054***	.781	.129
rs1416962		.321	.352	.16378	.39256	.4157	.38009	.566	***.019***
rs946755		.317	.344	.20073	.20147	≤.00001	.37434	.513	***.012***
rs6428352		.001	.003	…	≤.00001	≤.00001	…	…	…
rs800292	*CFH*	***.132***	***.232***	≤.00001	≤.00001	≤.00001	≤.00001	.437	.001
rs70620	*CFH*	.147	.173	.15602	≤.00001	≤.00001	.33122	.893	.333
rs1853883		***.630***	***.489***	≤.00001	≤.00001	≤.00001	≤.00001	.521	≤.001
rs1360558		.425	.397	.34842	.60377	***.01118***	.63012	.183	.296
rs955927		.416	.391	.36201	***.00833***	…	.65613	.065	.145
rs4350226		.055	.095	***.00182***	…	…	***.00183***	.171	.242
rs4752266	*GRK5*	.220	.223	.84131	.23223	.28973	***.03802***	.088	.475
rs915394	*GRK5*	.214	.187	.15214	.19235	***.00309***	.35594	***.028***	.643
rs1268947	*GRK5*	.112	.117	.97426	***.00969***	***.01031***	.97976	.052	.345
rs1537576	*GRK5*	.507	.433	***.01881***	***.01354***	***.03257***	***.0295***	***.006***	.251
rs2039488		.078	.115	***.01339***	.07877	…	.05075	***.004***	.609
rs1467813	*RGS10*	.286	.293	.63177	…	…	.71857	.539	.582
rs927427		.514	.464	.06936	.00003	.00002	.05976	.198	.577
rs4146894	*PLEKHA1*	***.598***	***.466***	≤.00001	≤.00001	.00001	≤.00001	***.008***	.802
rs1882907		.127	.187	***.00261***	.00013	.00006	***.00521***	.169	.172
rs760336	*PRSS11*	.395	.480	***.00469***	***.00126***	…	***.02036***	.232	.581
rs763720	*PRSS11*	.295	.212	.00053	…	…	***.00290***	.198	***.021***

Note.—The minor-allele frequency is reported for controls (estimated by counting) and families (estimated by Mendel, version 5). Allele frequencies that differed between controls and families by >0.1 are in bold italics. For the allele test, the two-SNP and three-SNP moving-window haplotype tests, and the genotype test from the CCREL, *P* values ≤.05 are in bold italics and *P* values ≤.001 are underlined. The moving-window haplotype *P* values correspond to the SNPs in the same row as the *P* value and the next one or two SNPs for the two- and three-SNP moving window, respectively. For GIST, with the use of NPL scores from chromosome 1 (NPL 1) and chromosome 10 (NPL 10), *P* values ≤.05 are in bold italics and *P* values ≤.001 are underlined. Blank spaces separate the three chromosomal regions corresponding to SNPs in and around *CFH, GRK5/RGS10,* and *PLEKHA1/LOC687715/PRSS11.*

those regions in which Tgfβ proteins play a regulatory role (De Luca et al. 2004). Oka and colleagues (2004) have shown that HtrA1 is capable of inhibiting the signaling of a number of Tgfβ family proteins, including Bmp4, Bmp2, and Tgfβ1, presumably by preventing receptor activation with a requirement for protease activity of the HtrA1 molecule. One clue as to the potential importance of these relationships for ARM comes from the studies of Hollborn et al. (2004), who found that human RPE cells in vitro experienced reduced proliferation in the presence of Tgfβ1 and Tgfβ2 and an increase in levels of collagen III and collagen IV transcripts. Normally, a rise in collagen III would activate HtrA1 and would lead to secondary inhibition of the effects of Tgfβ1. However, if the serine protease is less effective (because of either reduced synthesis or a nonfunctional mutation), then this regulatory pathway would be disrupted, leading to an overall reduction in the proliferation potential of the RPE cells, perhaps contributing to RPE atrophy or further changes that could lead to the development of ARM. The gradual reduction in solubility of type III collagen in Bruch membrane that has been observed with aging could also, in part, account for a general reduction in HtrA1 activity as an individual ages.

Both *PRSS11* and *PLEKHA1* are expressed in the retina, and a SAGE analysis of central and peripheral retina (Gene Expression Omnibus [GEO] expression data) indicates higher levels of transcripts of both genes in the central macula (more so for *PLEKHA1* than for *PRSS11*). Multiple studies (reported in GEO profiles) have shown that *PLEKHA1* expression is significantly induced in a variety of cell types in response to exposure to specific inflammatory cytokines. *PRSS11* has also been investigated as part of a microarray expression analysis of dermal fibroblasts that have been oxidatively challenged, in a comparison between normal individuals and patients with ARM. In that study, half of the ARM samples (9 of 18) had lower Htra1 expression levels than any of the normal samples. The lower levels

Table 6

CCREL, GIST, and Allele-Frequency Estimation for Locally Typed Families and Controls

		Frequency in		*P* Value for Test					
					Moving-Window Haplotype Test			GIST	
SNP	Gene	Families (n = 323)	Controls (n = 117)	Allele Test	With 2 SNPs	With 3 SNPs	Genotype Test	NPL 10	NPL 1
rs6658788		.563	.483	***.02200***	.00052	***.00162***	***.04920***	.319	.244
rs1538687		***.213***	***.342***	.00004	.00043	.00066	.00014	.652	.302
rs1416962		.299	.393	***.00597***	***.02623***	***.02051***	***.01819***	.442	***.041***
rs946755		.295	.380	***.01234***	***.01243***	≤.00001	***.04531***	.409	***.040***
rs6428352		.001	.004	…	≤.00001	≤.00001	…	…	…
rs800292	*CFH*	***.120***	***.269***	≤.00001	≤.00001	≤.00001	≤.00001	.315	***.014***
rs1061170	*CFH*	***.609***	***.310***	≤.00001	≤.00001	≤.00001	≤.00001	.895	.132
rs10922093	*CFH*	.210	.295	***.00693***	***.00175***	≤.00001	***.01723***	.360	.327
rs70620	*CFH*	.148	.150	.91163	≤.00001	≤.00001	.56770	.737	.356
rs1853883		***.633***	***.432***	≤.00001	≤.00001	≤.00001	≤.00001	.776	***.011***
rs1360558		.437	.389	.18014	.43576	***.02079***	.37993	.975	.488
rs955927		.433	.385	.15343	***.01037***	…	.36087	***.017***	.585
rs4350226		.050	.103	***.00312***	…	…	***.00373***	.228	.174
rs4752266	*GRK5*	.223	.226	.81772	.27748	.64917	.08279	.107	.453
rs915394	*GRK5*	.228	.209	.34489	.83219	.05560	.62183	***.049***	.320
rs1268947	*GRK5*	.117	.115	.81975	***.02748***	***.02192***	.78965	***.049***	.689
rs1537576	*GRK5*	.497	.419	***.02604***	***.02232***	.05636	.06334	***.012***	***.023***
rs2039488		.083	.115	.11177	.42428	…	.42399	***.025***	.358
rs1467813	*RGS10*	.293	.295	.86608	…	…	.85954	.506	.492
rs927427		.506	.487	.56710	.00056	.00083	.42264	.306	.625
rs4146894	*PLEKHA1*	***.611***	***.474***	.00004	.00012	.00053	.00024	***.006***	.737
rs12258692	*PLEKHA1*	.008	.000	…	.54750	.00018	…	…	…
rs4405249	*PLEKHA1*	.139	.158	.39378	.00026	***.00280***	.33118	***.003***	.345
rs1045216	*PLEKHA1*	***.289***	***.427***	.00004	.00036	.00001	.00026	.068	.825
rs1882907		.131	.184	***.01761***	***.00140***	***.01099***	***.04401***	***.017***	.372
rs10490923	*LOC387715*	.089	.141	***.02112***	.05024	≤.00001	***.03415***	.086	.251
rs2736911	*LOC387715*	.121	.119	.71668	≤.00001	≤.00001	.64230	.312	.968
rs10490924	*LOC387715*	***.475***	***.193***	≤.00001	≤.00001	≤.00001	≤.00001	***.018***	.327
rs11538141	*PRSS11*	.004	.005	…	***.00726***	***.01676***	…	…	…
rs760336	*PRSS11*	***.373***	***.474***	***.00527***	***.01386***	.00036	***.01396***	.479	.683
rs763720	*PRSS11*	.296	.226	***.01645***	.00016	…	***.03899***	.305	.451
rs1803403	*PRSS11*	.118	.030	.00009	…	…	.00022	.714	.778

Note.—The minor-allele frequency is reported for controls (estimated by counting) and families (estimated by Mendel, version 5). Allele frequencies that differed between controls and families by >0.1 are in bold italics. For the allele test, the two-SNP and three-SNP moving-window haplotype tests, and the genotype test from the CCREL, *P* values ≤.05 are in bold italics and *P* values ≤.001 are underlined. The moving-window haplotype *P* values correspond to the SNPs in the same row as the *P* value and the next one or two SNPs for the two- and three-SNP moving window, respectively. For GIST, with the use of NPL scores from chromosome 1 (NPL 1) and chromosome 10 (NPL 10), *P* values ≤.05 are in bold italics and *P* values ≤.001 are underlined. Locally typed SNPs are in bold italics. Blank spaces separate the three chromosomal regions corresponding to SNPs in and around *CFH, GRK5/RGS10,* and *PLEKHA1/LOC687715/PRSS11.*

of Htra1 in nonocular tissues of patients with ARM would suggest that this is an intrinsic difference in the biology of these patients, compared with that of normal individuals, and is not a consequence of degenerative changes in the eye.

Several lines of evidence support the *GRK5/RGS10* locus. The peak of our S_{all} multipoint curve is directly over *GRK5,* and our largest two-point S_{all} = 3.86 (*rs555938*) is only 206 kb centromeric of *GRK5*. The *P* values for the GIST analysis of the *GRK5/RGS10* CIDR data were .004 and .006, which are even smaller than the *P* value for the SNP within *PLEKHA1* (*P* = .008). By use of our locally genotyped sample, the GIST *P* value for the *GRK5* locus was .012, which is comparable to the *P* value that we found for the Y402H variant in *CFH* (*P* = .011). However, the CCREL analyses were not very significant for the *GRK5* SNPs, and the ORs were mostly nonsignificant.

On the basis of biological evidence, *GRK5* is a reasonable ARM candidate gene, given its role in modulating neutrophil responsiveness to chemoattractants and its interactions with the Toll 4 receptor (Haribabu

Table 7

Results of Fitting Two-Locus Models by Logistic Regression

The table is available in its entirety in the online edition of *The American Journal of Human Genetics*.

and Snyderman 1993; Fan and Malik 2003), which has also been implicated in ARM (Zareparsi et al. 2005*b*). The retinal or RPE expression of *GRK5* is not especially relevant to the argument of causality, because it would be the expression and function of *GRK5* in migrating lymphocytes and macrophages that would be crucial to its role in the immune and/or inflammatory pathways that may be pathogenic in ARM. The strongest GIST results occur at *rs2039488*, which is located between *GRK5* and *RGS10*, 3′ of the ends of both genes. Several other SNPs within *GRK5* also have small GIST *P* values, whereas the *RGS10* SNP has a nonsignificant GIST *P* value. However, we cannot completely exclude the possibility that there is a SNP within *RGS10* that is in strong LD with *rs2039488*.

RGS10 is one of a family of G protein–coupled receptors that has been implicated in chemokine-induced lymphocyte migration (Moratz et al. 2004) and whose expression in dendritic cells (which have been identified in ARM-related drusen deposits) is modified by the Toll-like signaling pathway (Shi et al. 2004). *RGS10* and *GRK5* expression in the same microarray study of oxidatively stressed dermal fibroblasts in patients with ARM and control subjects showed minor fluctuations among the samples but no clear differences between the controls and affected individuals. This does not necessarily lower the potential for these genes being involved in ARM, since the dermal fibroblasts lack the cell populations that would be expected to have modulation of *RGS10*- and/or *GRK5*-related proteins.

Table 8

ORs, ARs, and Simulated *P* Values from χ^2 Test with 10,000 Replicates

		Dominant ([RR+RN] vs. NN)				Heterozygotes (RR vs. NN)		Recessive (RR vs. [RN+NN])				Homozygotes (RR vs. NN)	
SNP (Allele)	Gene	OR	95% CI	AR	*P*	OR	AR	OR	95% CI	AR	*P*	OR	AR
rs6658788 (2)		.83	.57–1.22	−14.04	.3909	1.09	2.69	1.01	.68–1.5	.21	1	.88	−5.92
rs1538687 (2)		***.68***	.49–.95	***−19.38***	.023	***.5***	***−11.74***	***.42***	.23–.78	***−6.52***	.0068	***.38***	***−12.42***
rs1416962 (2)		.84	.6–1.18	−10.02	.3418	.89	−2.57	.82	.49–1.38	−2.31	.5002	.77	−5.74
rs946755 (2)		.8	.57–1.13	−12.52	.232	1	.04	.9	.53–1.52	−1.24	.7816	.81	−4.34
rs6428352 (2)		…	…	…	…	…	…	…	…	…	…	…	…
rs800292 (1)	*CFH*	.43	.3–.62	−30.01	<.0001	.48	−23.85	.15	.05–.45	−4.98	.0001	.12	−8.19
rs1061170 (2)	*CFH*	5.29	3.35–8.35	68.2	<.0001	***2.66***	***28.55***	4.57	2.48–8.42	30.06	<.0001	10.05	63.72
rs10922093 (1)	*CFH*	***.59***	.39–.88	***−25.61***	.0111	***.63***	***−19.65***	.5	.24–1.04	−4.98	.0736	***.41***	***−10.14***
rs70620 (1)	*CFH*	.83	.57–1.19	−5.64	.3366	.85	−4.29	.67	.27–1.68	−1.3	.4525	.64	−1.93
rs1853883 (2)		2.67	1.78–4.01	54.41	<.0001	***1.65***	***19.21***	2.08	1.43–3.02	22.06	.0003	3.55	55.04
rs1360558 (1)		1.16	.82–1.65	9.12	.414	1.1	5.39	1.25	.8–1.96	3.94	.3774	1.32	9.01
rs955927 (2)		1.13	.79–1.6	7.5	.5303	1.28	6.35	1.31	.83–2.08	4.53	.2588	1.36	9.38
rs4350226 (2)		***.51***	.32–.81	***−9.68***	.0038	.27	−4.76	.16	.01–1.74	−.95	.142	.14	−1.16
rs4752266 (2)	*GRK5*	.88	.62–1.23	−5.57	.4325	***3.27***	***10.68***	***2.81***	.98–8.04	***3.89***	.0457	2.56	5.51
rs915394 (2)	*GRK5*	1.28	.9–1.82	8.91	.1543	1.35	2.73	1.56	.58–4.14	1.53	.3892	1.68	2.72
rs1268947 (2)	*GRK5*	1.05	.7–1.57	1.06	.841	1.24	1.82	1.27	.35–4.55	.45	.7761	1.28	.58
rs1537576 (2)	*GRK5*	***1.59***	1.11–2.29	***27.95***	.0109	.89	−3.74	1.08	.71–1.62	1.59	.7579	1.47	15.14
rs2039488 (2)		.7	.45–1.07	−6.5	.1067	.23	−11.98	***.19***	.04–.79	***−2.33***	.0242	***.18***	***−2.85***
rs1467813 (1)	*RGS10*	.96	.69–1.35	−1.84	.8645	1.01	.42	.77	.42–1.38	−2.27	.4265	.77	−3.76
rs927427 (1)		1.09	.74–1.62	6.57	.6172	.94	−4.66	***1.67***	1.09–2.56	***10.73***	.0201	1.6	19.91
rs4146894 (1)	*PLEKHA1*	2.22	1.49–3.31	46.78	.0002	***1.77***	***33.08***	2.21	1.49–3.29	20.46	<.0001	3.31	49.88
rs12258692 (2)	*PLEKHA1*	…	…	…	…	…	…	…	…	…	…	…	…
rs4405249 (1)	*PLEKHA1*	.62	.33–1.15	−12.96	.1692	.61	−12.69	.87	.1–7.56	−.23	1	.77	−.57
rs1045216 (2)	*PLEKHA1*	.48	.32–.74	−51.23	.0005	***.49***	***−18.27***	.37	.21–.65	−14.3	.0003	.28	−35.68
rs1882907 (2)		***.58***	.4–.84	***−16.73***	.0026	.44	−5.79	***.31***	.1–.97	***−2.37***	.0438	***.27***	***−3.65***
rs10490923 (2)	*LOC387715*	***.53***	.31–.9	***−13.27***	.0239	.34	−9.01	.22	.04–1.09	−2.51	.0809	.2	−3.32
rs2736911 (2)	*LOC387715*	.72	.42–1.21	−6.92	.2552	1.47	1.99	1.1	.13–9.53	.1	1	1.03	.04
rs10490924 (2)	*LOC387715*	5.03	3.2–7.91	57.11	<.0001	***2.72***	***22.76***	5.75	2.46–13.46	21.2	<.0001	10.57	42.71
rs11538141 (2)	*PRSS11*	…	…	…	…	…	…	…	…	…	…	…	…
rs760336 (2)	*PRSS11*	***.64***	.44–.93	***−35.37***	.013	.8	−6.95	.69	.46–1.03	−7.95	.0773	***.55***	***−26.43***
rs763720 (1)	*PRSS11*	***1.69***	1.2–2.38	***21.24***	.0018	***1.55***	***16.95***	***2.63***	1.1–6.25	***5.17***	.0277	***3.16***	***10.14***
rs1803403 (1)	*PRSS11*	***2.98***	1.25–7.06	***10.51***	.0093	***2.98***	***10.51***	…	…	…	…	…	…

Note.—Type A–affected individuals are compared with controls. OR and AR values are underlined if corresponding *P* values are ⩽.001 and are in bold italics if *P* values are ⩽.05. Allele denotes the risk allele (minor allele in controls). RR = homozygotes for the risk allele; RN = heterozygotes for the risk allele; NN = homozygotes for the normal allele. Locally typed SNPs are in bold italics. Blank spaces separate the three chromosomal regions corresponding to SNPs in and around *CFH*, *GRK5/RGS10*, and *PLEKHA1/LOC687715/PRSS11*.

Table 9

ORs and ARs from Analysis of ARM Subtypes

The table is available in its entirety in the online edition of *The American Journal of Human Genetics*.

We have attempted to look at potential interactions between the high-risk alleles within the *PLEKHA1/LOC387715* and *GRK5/RGS10* loci with respect to *CFH* on chromosome 1. This is perhaps the first report to use GIST to examine these interactions, and we found no evidence that the NPL data on chromosome 1 could be accounted for by the SNP data on chromosome 10. Conversely, we found no such associations between the NPL data on chromosome 10 and the SNP data from the *CFH* alleles. Logistic regression analysis also failed to identify an interaction, and it appears that a simple additive risk model is the most parsimonious. We have performed some initial logistic analyses that include exposure to smoking. These analyses were initiated because of the previous suggestion of an interaction between smoking and the biology of complement factor H (Esparza-Gordillo et al. 2004) and because of our prior studies, which found an interaction between smoking and the locus on chromosome 10q26 (Weeks et al. 2004). To date, we have found no strong interaction between smoking and either *CFH* or *PLEKHA1/LOC387715,* but we are still exploring a possible interaction with the *GRK5/RGS10* locus and different modeling strategies.

We also examined the associations of ARM subphenotypes with the SNPs on chromosomes 1 and 10 (table 9). We found no major differences in the ORs for the presence of either GA or CNV, which suggests that these ARM loci contribute to a common pathogenic pathway that can give rise to either end-stage form of the disease. This does not exclude the possibility that there are other as-yet-undescribed genetic loci that may confer specific risk of GA or CNV development separately.

In summary, these SNP-based linkage and association studies illustrate both the power and the limitation of such methods to identify the causative alleles and genes underlying ARM susceptibility. These genetic approaches allow us to consider genes and their variants that may contribute to disease, whether or not there is tissue-specific expression. Through high-density SNP genotyping, we have narrowed the list of candidate genes within the linkage peak found on chromosome 10q26, from hundreds of genes to primarily *GRK5* and *PLEKHA1,* but we cannot completely exclude possible roles for *RGS10* and/or *PRSS11* and *LOC387715*. Additional genotyping of nonsynonymous 3′ SNPs within the *GRK5* gene may help to further discriminate between *GRK5* and *RGS10,* but it may not establish a definitive assignment of causality. Replication by other studies (as done in the case of *CFH*) may allow the attention to be focused on a single gene in future studies of ARM pathology, but there is also the distinct possibility that we will be unable to achieve further resolution with association studies or to clearly establish whether there are more than two genes responsible for ARM susceptibility on chromosome 10q26. However, it is now well within the capabilities of molecular biologists to investigate the potential role of each of these candidate genes in mouse models of ARM and to address the issue of a causal role in disease pathogenesis. Association studies are an incredibly powerful means of testing hypotheses of genetic contributions to disease, but, except in the most extreme cases, they cannot provide definitive answers, even when there are impressive *P* values.

Acknowledgments

We gratefully acknowledge the many individuals and family members who participated as research subjects, as well as their eye care providers for this study. We also wish to express our thanks to our current and past clinical research team: E. Adams, C. Baic, L. R. Barnes, F. Bivins, M. Blagodatny, A. Burchis, I. Cantillo, J. Green, B. Gur, K. Hendricks, C. Klump, S. Pope, M. Shaffer-Gordon, H. Sheth, S. Ward, and B. Zhu, and to our laboratory research staff: Y. Demirci (who tested for retinal expression of the three candidate genes), H. Brockway, S. Deslouches, and B. Rigatti. Illumina-based SNP genotyping services were provided by the Center for Inherited Disease Research, which is fully funded through federal contract N01-HG-65403 from the National Institutes of Health to The Johns Hopkins University. This study was supported by National Eye Institute grant R01EY009859 (to M.B.G.); The Steinbach Foundation, New York (to M.B.G.); Research to Prevent Blindness, New York (Senior Scientist Investigator Award to M.B.G.); and the Eye and Ear Foundation of Pittsburgh (to M.B.G.).

Web Resources

The URLs for data presented herein are as follows:

Online Mendelian Inheritance in Man (OMIM), http://www.ncbi.nlm.nih.gov/Omim/ (for ARMD-1, *CFH, PLEKHA1, PRSS11, GRK5,* and *RGS10*)

Division of Statistical Genetics, http://watson.hgen.pitt.edu/ (for Mega2)

The R Project for Statistical Computing, http://www.r-project.org/ (for R statistical software)

References

Abecasis GR, Cherny SS, Cookson WO, Cardon LR (2002) Merlin—rapid analysis of dense genetic maps using sparse gene flow trees. Nat Genet 30:97–101

Abecasis GR, Yashar BM, Zhao Y, Ghiasvand NM, Zareparsi

S, Branham KE, Reddick AC, Trager EH, Yoshida S, Bahling J, Filippova E, Elner S, Johnson MW, Vine AK, Sieving PA, Jacobson SG, Richards JE, Swaroop A (2004) Age-related macular degeneration: a high-resolution genome scan for susceptibility loci in a population enriched for late-stage disease. Am J Hum Genet 74:482–494

Barrett JC, Fry B, Maller J, Daly MJ (2005) Haploview: analysis and visualization of LD and haplotype maps. Bioinformatics 21:263–265

Browning SR, Briley JD, Briley LP, Chandra G, Charnecki JH, Ehm MG, Johansson KA, Jones BJ, Karter AJ, Yarnall DP, Wagner MJ (2005) Case-control single-marker and haplotypic association analysis of pedigree data. Genet Epidemiol 28:110–122

Conley YP, Thalamuthu A, Jakobsdottir J, Weeks DE, Mah T, Ferrell RE, Gorin MB (2005) Candidate gene analysis suggests a role for fatty acid biosynthesis and regulation of the complement system in the etiology of age-related maculopathy. Hum Mol Genet 14:1991–2002

De Luca A, De Falco M, De Luca L, Penta R, Shridhar V, Baldi F, Campioni M, Paggi MG, Baldi A (2004) Pattern of expression of HtrA1 during mouse development. J Histochem Cytochem 52:1609–1617

Dowler S, Currie RA, Campbell DG, Deak M, Kular G, Downes CP, Alessi DR (2000) Identification of pleckstrin-homology-domain-containing proteins with novel phosphoinositide-binding specificities. Biochem J 351:19–31

Edwards AO, Ritter R III, Abel KJ, Manning A, Panhuysen C, Farrer LA (2005) Complement factor H polymorphism and age-related macular degeneration. Science 308:421–424

Esparza-Gordillo J, Soria JM, Buil A, Almasy L, Blangero J, Fontcuberta J, Rodriguez de Cordoba S (2004) Genetic and environmental factors influencing the human factor H plasma levels. Immunogenetics 56:77–82

Fan J, Malik AB (2003) Toll-like receptor-4 (TLR4) signaling augments chemokine-induced neutrophil migration by modulating cell surface expression of chemokine receptors. Nat Med 9:315–321

Fisher SA, Abecasis GR, Yashar BM, Zareparsi S, Swaroop A, Iyengar SK, Klein BE, Klein R, Lee KE, Majewski J, Schultz DW, Klein ML, Seddon JM, Santangelo SL, Weeks DE, Conley YP, Mah TS, Schmidt S, Haines JL, Pericak-Vance MA, Gorin MB, Schulz HL, Pardi F, Lewis CM, Weber BH (2005) Meta-analysis of genome scans of age-related macular degeneration. Hum Mol Genet 14:2257–2264

Gudbjartsson DF, Jonasson K, Frigge ML, Kong A (2000) Allegro, a new computer program for multipoint linkage analysis. Nat Genet 25:12–13

Hageman GS, Anderson DH, Johnson LV, Hancox LS, Taiber AJ, Hardisty LI, Hageman JL, et al (2005) A common haplotype in the complement regulatory gene factor H (*HF1/CFH*) predisposes individuals to age-related macular degeneration. Proc Natl Acad Sci USA 102:7227–7232

Hageman GS, Luthert PJ, Victor Chong NH, Johnson LV, Anderson DH, Mullins RF (2001) An integrated hypothesis that considers drusen as biomarkers of immune-mediated processes at the RPE-Bruch's membrane interface in aging and age-related macular degeneration. Prog Retin Eye Res 20:705–732

Hageman GS, Mullins RF (1999) Molecular composition of drusen as related to substructural phenotype. Mol Vis 5:28

Haines JL, Hauser MA, Schmidt S, Scott WK, Olson LM, Gallins P, Spencer KL, Kwan SY, Noureddine M, Gilbert JR, Schnetz-Boutaud N, Agarwal A, Postel EA, Pericak-Vance MA (2005) Complement factor H variant increases the risk of age-related macular degeneration. Science 308: 419–421

Haribabu B, Snyderman R (1993) Identification of additional members of human G-protein-coupled receptor kinase multigene family. Proc Natl Acad Sci USA 90:9398–9402

Hollborn M, Reichenbach A, Wiedemann P, Kohen L (2004) Contrary effects of cytokines on mRNAs of cell cycle- and ECM-related proteins in hRPE cells in vitro. Curr Eye Res 28:215–223

Huang Q, Shete S, Amos CI (2004) Ignoring linkage disequilibrium among tightly linked markers induces false-positive evidence of linkage for affected sib pair analysis. Am J Hum Genet 75:1106–1112

Iyengar SK, Song D, Klein BE, Klein R, Schick JH, Humphrey J, Millard C, Liptak R, Russo K, Jun G, Lee KE, Fijal B, Elston RC (2004) Dissection of genomewide-scan data in extended families reveals a major locus and oligogenic susceptibility for age-related macular degeneration. Am J Hum Genet 74:20–39

Johnson LV, Leitner WP, Staples MK, Anderson DH (2001) Complement activation and inflammatory processes in drusen formation and age related macular degeneration. Exp Eye Res 73:887–896

Johnson LV, Ozaki S, Staples MK, Erickson PA, Anderson DH (2000) A potential role for immune complex pathogenesis in drusen formation. Exp Eye Res 70:441–449

Kenealy SJ, Schmidt S, Agarwal A, Postel EA, De La Paz MA, Pericak-Vance MA, Haines JL (2004) Linkage analysis for age-related macular degeneration supports a gene on chromosome 10q26. Mol Vis 10:57–61

Klein ML, Schultz DW, Edwards A, Matise TC, Rust K, Berselli CB, Trzupek K, Weleber RG, Ott J, Wirtz MK, Acott TS (1998) Age-related macular degeneration: clinical features in a large family and linkage to chromosome 1q. Arch Ophthalmol 116:1082–1088

Klein RJ, Zeiss C, Chew EY, Tsai J-Y, Richard S, Sackler RS, Chad Haynes C, Henning AK, SanGiovanni JP, Mane SM, Mayne ST, Bracken MB, Ferris FL, Ott J, Barnstable C, Hoh J (2005) Complement factor H polymorphism in age-related macular degeneration. Science 308:385–389

Kong X, Murphy K, Raj T, He C, White PS, Matise TC (2004) A combined linkage-physical map of the human genome. Am J Hum Genet 75:1143–1148

Lange K, Cantor RM, Horvath S, Perola M, Sabatti C, Sinsheimer J, Sobel E (2001) MENDEL version 4.0: a complete package for the exact genetic analysis of discrete traits in pedigree and population data sets. Am J Hum Genet Suppl 69:A1886

Li C, Scott LJ, Boehnke M (2004) Assessing whether an allele can account in part for a linkage signal: the Genotype-IBD Sharing Test (GIST). Am J Hum Genet 74:418–431

Majewski J, Schultz DW, Weleber RG, Schain MB, Edwards AO, Matise TC, Acott TS, Ott J, Klein ML (2003) Age-

related macular degeneration—a genome scan in extended families. Am J Hum Genet 73:540–550

Moratz C, Harrison K, Kehrl JH (2004) Regulation of chemokine-induced lymphocyte migration by RGS proteins. Methods Enzymol 389:15–32

Mukhopadhyay N, Almasy L, Schroeder M, Mulvihill WP, Weeks DE (2005) Mega2: data-handling for facilitating genetic linkage and association analyses. Bioinformatics 21: 2556–2557

Mukhopadhyay N, Buxbaum SG, Weeks DE (2004) Comparative study of multipoint methods for genotype error detection. Hum Hered 58:175–189

Mullins RF, Russell SR, Anderson DH, Hageman GS (2000) Drusen associated with aging and age-related macular degeneration contain proteins common to extracellular deposits associated with atherosclerosis, elastosis, amyloidosis, and dense deposit disease. FASEB J 14:835–846

Murwantoko, Yano M, Ueta Y, Murasaki A, Kanda H, Oka C, Kawaichi M (2004) Binding of proteins to the PDZ domain regulates proteolytic activity of HtrA1 serine protease. Biochem J 381:895–904

North BV, Curtis D, Sham PC (2005) Application of logistic regression to case-control association studies involving two causative loci. Hum Hered 59:79–87

O'Connell JR, Weeks DE (1998) PedCheck: a program for identifying genotype incompatibilities in linkage analysis. Am J Hum Genet 63:259–266

Oka C, Tsujimoto R, Kajikawa M, Koshiba-Takeuchi K, Ina J, Yano M, Tsuchiya A, Ueta Y, Soma A, Kanda H, Matsumoto M, Kawaichi M (2004) HtrA1 serine protease inhibits signaling mediated by Tgfβ family proteins. Development 131:1041–1053

R Development Core Team (2004) R: a language and environment for statistical computing. R Foundation for Statistical Computing, Vienna

Rinaldo A, Bacanu SA, Devlin B, Sonpar V, Wasserman L, Roeder K (2005) Characterization of multilocus linkage disequilibrium. Genet Epidemiol 28:193–206

Santangelo SL, Yen C-H, Haddad S, Fagerness J, Huang C, Seddon JM (2005) A discordant sib-pair linkage analysis of age-related macular degeneration. Ophthalmic Genet 26: 61–67

Schaid DJ, McDonnell SK, Wang L, Cunningham JM, Thibodeau SN (2002) Caution on pedigree haplotype inference with software that assumes linkage equilibrium. Am J Hum Genet 71:992–995

Schick JH, Iyengar SK, Klein BE, Klein R, Reading K, Liptak R, Millard C, Lee KE, Tomany SC, Moore EL, Fijal BA, Elston RC (2003) A whole-genome screen of a quantitative trait of age-related maculopathy in sibships from the Beaver Dam Eye Study. Am J Hum Genet 72:1412–1424

Schmidt S, Scott WK, Postel EA, Agarwal A, Hauser ER, De La Paz MA, Gilbert JR, Weeks DE, Gorin MB, Haines JL, Pericak-Vance MA (2004) Ordered subset linkage analysis supports a susceptibility locus for age-related macular degeneration on chromosome 16p12. BMC Genet 5:18

Seddon JM, Santangelo SL, Book K, Chong S, Cote J (2003) A genomewide scan for age-related macular degeneration provides evidence for linkage to several chromosomal regions. Am J Hum Genet 73:780–790

Shi GX, Harrison K, Han SB, Moratz C, Kehrl JH (2004) Toll-like receptor signaling alters the expression of regulator of G protein signaling proteins in dendritic cells: implications for G protein-coupled receptor signaling. J Immunol 172: 5175–5184

Weeks DE, Conley YP, Mah TS, Paul TO, Morse L, Ngo-Chang J, Dailey JP, Ferrell RE, Gorin MB (2000) A full genome scan for age-related maculopathy. Hum Mol Genet 9:1329–1349

Weeks DE, Conley YP, Tsai HJ, Mah TS, Schmidt S, Postel EA, Agarwal A, Haines JL, Pericak-Vance MA, Rosenfeld PJ, Paul TO, Eller AW, Morse LS, Dailey JP, Ferrell RE, Gorin MB (2004) Age-related maculopathy: a genomewide scan with continued evidence of susceptibility loci within the 1q31, 10q26, and 17q25 regions. Am J Hum Genet 75: 174–189

Zareparsi S, Branham KE, Li M, Shah S, Klein RJ, Ott J, Hoh J, Abecasis GR, Swaroop A (2005*a*) Strong association of the Y402H variant in complement factor H at 1q32 with susceptibility to age-related macular degeneration. Am J Hum Genet 77:149–153

Zareparsi S, Buraczynska M, Branham KE, Shah S, Eng D, Li M, Pawar H, Yashar BM, Moroi SE, Lichter PR, Petty HR, Richards JE, Abecasis GR, Elner VM, Swaroop A (2005*b*) Toll-like receptor 4 variant D299G is associated with susceptibility to age-related macular degeneration. Hum Mol Genet 14:1449–1455